8

Design of a Humanoid Robot Eye

Giorgio Cannata*, Marco Maggiali**
**University of Genova*
Italy
*** Italian Institute of Technology*
Italy

1. Introduction

This chapter addresses the design of a robot eye featuring the mechanics and motion characteristics of a human one. In particular the goal is to provide guidelines for the implementation of a tendon driven robot capable to emulate saccadic motions.
In the first part of this chapter the physiological and mechanical characteristics of the eye-plant[1] in humans and primates will be reviewed. Then, the fundamental motion strategies used by humans during saccadic motions will be discussed, and the mathematical formulation of the relevant *Listing's Law* and *Half-Angle Rule*, which specify the geometric and kinematic characteristics of ocular saccadic motions, will be introduced.
From this standpoint a simple model of the eye-plant will be described. In particular it will be shown that this model is a good candidate for the implementation of Listing's Law on a purely mechanical basis, as many physiologists believe to happen in humans. Therefore, the proposed eye-plant model can be used as a reference for the implementation of a robot emulating the actual mechanics and actuation characteristics of the human eye.
The second part of this chapter will focus on the description of a first prototype of fully embedded robot eye designed following the guidelines provided by the eye-plant model. Many eye-head robots have been proposed in the past few years, and several of these systems have been designed to support and rotate one or more cameras about independent or coupled *pan-tilt* axes. However, little attention has been paid to emulate the actual mechanics of the eye, although theoretical investigations in the area of modeling and control of human-like eye movements have been presented in the literature (Lockwood et al., 1999; Polpitiya & Ghosh, 2002; Polpitiya & Ghosh, 2003; Polpitiya et al., 2004).
Recent works have focused on the design of embedded mechatronic robot eye systems (Gu et al., 2000; Albers et al., 2003; Pongas et al., 2004). In (Gu et al., 2000), a prosthetic implantable robot eye concept has been proposed, featuring a single degree-of-freedom. Pongas et al., (Pongas et al., 2004) have developed a mechanism which actuates a CMOS micro-camera embedded in a spherical support. The system has a single degree-of-freedom, and the spherical shape of the eye is a purely aesthetical detail; however, the mechatronic approach adopted has addressed many important engineering issues and led to a very

[1] By eye-plant we mean the eye-ball and all the mechanical structure required for its actuation and support.

Source: Humanoid Robots, New Developments, Book edited by: Armando Carlos de Pina Filho
ISBN 978-3-902613-02-8, pp.582, I-Tech, Vienna, Austria, June 2007

interesting system. In the prototype developed by Albers et al., (Albers et al., 2003) the design is more *humanoid*. The robot consists of a sphere supported by *slide bearings* and moved by a stud constrained by two gimbals. The relevance of this design is that it actually exploits the spherical shape of the eye; however, the types of ocular motions which could be generated using this system have not been discussed.
In the following sections the basic mechanics of the eye-plant in humans will be described and a quantitative geometric model introduced. Then, a first prototype of a tendon driven robot formed by a sphere hold by a low friction support will be discussed. The second part of the chapter will described some of the relevant issues faced during the robot design.

2. The human eye

The human eye has an almost spherical shape and is hosted within a cavity called *orbit*; it has an average diameter ranging between *23 mm* and *23.6 mm*, and weighs between *7 g* and *9 g*. The eye is actuated by a set of six *extra-ocular muscles* which allow the eye to rotate about its centre with negligible translations (Miller & Robinson, 1984; Robinson, 1991).
The rotation range of the eye can be approximated by a cone, formed by the admissible directions of fixation, with an average width of about 76 *deg* (Miller & Robinson, 1984). The action of the extra-ocular muscles is capable of producing accelerations up to *20.000 deg sec*$^{-2}$ allowing to reach angular velocities up to *800 deg sec*$^{-1}$ (Sparks, 2002).
The extra-ocular muscles are coupled in *agonostic/antagonistic* pairs, and classified in two groups: *recti* (*medial/lateral* and *superior/inferior*), and *obliqui* (*superior/inferior*). The four recti muscles have a common origin in the bottom of the orbit (*annulus of Zinn*); they diverge and run along the eye-ball up to their *insertion points* on the *sclera* (the eye-ball surface). The insertion points form an angle of about *55 deg* with respect to the optical axis and are placed symmetrically (Miller & Robinson, 1984; Koene & Erkelens, 2004). (Fig. 1, gives a qualitative idea of the placement of the four recti muscles.) The obliqui muscles have a more complex path within the orbit: they produce actions almost orthogonal to those generated by the recti, and are mainly responsible for the torsion of the eye about its optical axis. The superior oblique has its origin from the annulus of Zinn and is routed through a connective sleeve called *troclea*; the inferior oblique starts from the side of the orbit and is routed across the orbit to the eye ball.

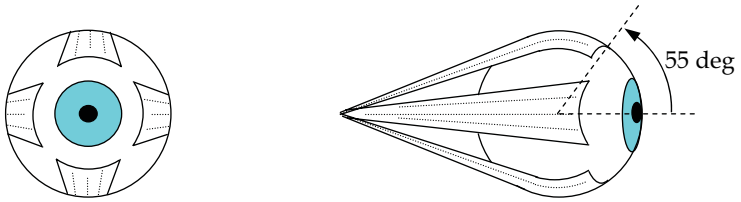

Fig. 1. Frontal and side view of the eye: qualitative placement of recti muscles.

Recent anatomical and physiological studies have suggested that the four recti have an important role for the implementation of saccadic motions which obey to the so called *Listing's Law*. In fact, it has been found that the path of the recti muscles within the orbit is constrained by soft connective tissue (Koornneef, 1974; Miller, 1989, Demer et al., 1995, Clark et al. 2000, Demer et al., 2000), named *soft-pulleys*. The role of the soft-pulleys to

generate ocular motions compatible with Listing's Law in humans and primates is still debated (Hepp, 1994; Raphan, 1998; Porrill et al., 2000; Wong et al., 2002; Koene & Erkelens 2004; Angelaki, 2004); however, analytical and simulation studies suggest that the implementation of Listing's Law on a mechanical basis is feasible (Polpitiya, 2002; Polpitiya, 2003; Cannata et al., 2006; Cannata & Maggiali, 2006).

3. Saccadic motions and Listing's Law

The main goal of the section is to introduce saccades and provide a mathematical formulation of the geometry and kinematics of saccadic motions, which represent the starting point for the development of models for their implementation.

Saccadic motions consist of rapid and sudden movements changing the direction of fixation of the eye. Saccades have duration of the order of a few hundred milliseconds, and their high speed implies that these movements are open loop with respect to visual feedback (Becker, 1991); therefore, the control of the rotation of the eye during a saccade must depend only on the mechanical and actuation characteristics of the eye-plant. Furthermore, the lack of any stretch or proprioceptive receptor in extra-ocular muscles (Robinson, 1991), and the unclear role of other sensory feedback originated within the orbit (Miller & Robinson, 1984), suggest that the implementation of Listing's Law should have a strong mechanical basis.

Although saccades are apparently controlled in open-loop, experimental tests show that they correspond to regular eye orientations. In fact, during saccades the eye orientation is determined by a basic principle known as Listing's Law, which establishes the amount of eye torsion for each direction of fixation. Listing's Law has been formulated in the mid of the 19th century, but it has been experimentally verified on humans and primates only during the last 20 years (Tweed & Vilis, 1987; Tweed & Vilis, 1988; Tweed & Vilis, 1990; Furman & Schor, 2003).

Listing's Law states that there exists a specific orientation of the eye (with respect to a head fixed reference frame $<h> = \{\boldsymbol{h}_1,\boldsymbol{h}_2,\boldsymbol{h}_3\}$), called *primary position*. During saccades any physiological orientation of the eye (described by the frame $<e> = \{\boldsymbol{e}_1,\boldsymbol{e}_2,\boldsymbol{e}_3\}$), with respect to the primary position, can be expressed by a unit quaternion q whose (unit) rotation axis, $\boldsymbol{v}$, always belongs to a head fixed plane, $\mathcal{L}$. The normal to plane $\mathcal{L}$ is the eye's direction of fixation at the primary position. Without loss of generality we can assume that $\boldsymbol{e}_3$ is the fixation axis of the eye, and that $<h> \equiv <e>$ at the primary position: then, $\mathcal{L} = span\{\boldsymbol{h}_1, \boldsymbol{h}_2\}$. Fig. 2 shows the geometry of Listing compatible rotations.

In order to ensure that $\boldsymbol{v} \in \mathcal{L}$ at any time, the eye's angular velocity ω, must belong to a plane $\mathcal{P}_\omega$, passing through $\boldsymbol{v}$, whose normal, $\boldsymbol{n}_\omega$, forms an angle of $\theta/2$ with the direction of fixation at the primary position, see Fig. 3. This property, directly implied by Listing's Law, is usually called *Half Angle Rule*, (Haslwanter, 1995). During a generic saccade the plane $\mathcal{P}_\omega$ is rotating with respect to both the head and the eye due to its dependency from $\boldsymbol{v}$ and θ. This fact poses important questions related to the control mechanisms required to implement the Listing's Law, also in view of the fact that there is no evidence of sensors in the eye-plant capable to detect how $\mathcal{P}_\omega$ is oriented. Whether Listing's Law is implemented in humans and primates on a mechanical basis, or it requires an active feedback control action, processed by the brain, has been debated among neuro-physiologists in the past few years. The evidence of the so called soft pulleys, within the orbit, constraining the extra ocular muscles, has

suggested that the mechanics of the eye plant could have a significant role in the implementation of Half Angle Rule and Listing's Law (Quaia & Optican, 1998; Raphan 1998; Porril et al., 2000; Koene & Erkelens, 2004), although counterexamples have been presented in the literature (Hepp, 1994; Wong et al., 2002).

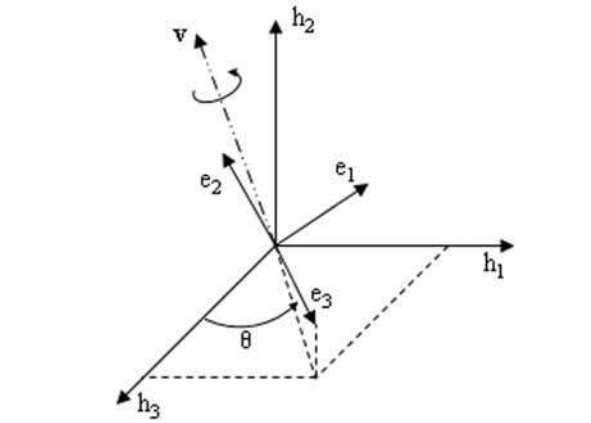

Fig. 2 Geometry of Listing compatible rotations. The finite rotation of the eye fixed frame <*e*>, with respect to <*h*> is described by a vector $\boldsymbol{v}$ always orthogonal to $\boldsymbol{h_3}$.

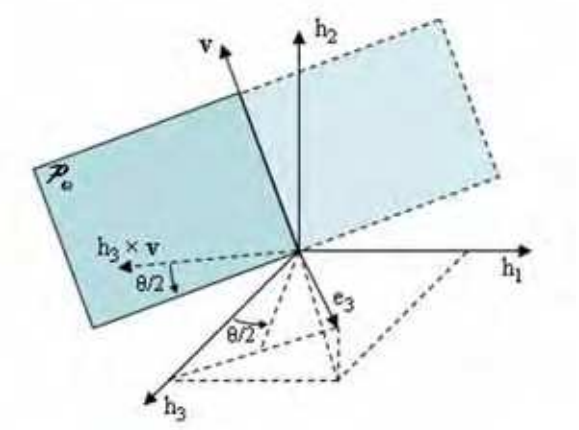

Fig. 3. *Half Angle Rule* geometry. The eye's angular velocity must belong to the plane $\mathscr{P}_v$ passing through axis $\boldsymbol{v}$.

4. Eye Model

The eye in humans has an almost spherical shape and is actuated by six extra-ocular muscles. Each extra-ocular muscle has an insertion point on the sclera, and is connected with the bottom of the orbit at the other end. Accordingly to the rationale proposed in (Haslwanter, 2002; Koene & Erkelens, 2004), only the four rectii extra-ocular muscles play a significant role during saccadic movements. In (Lockwood et al., 1989), a complete 3D model of the eye plant including a non linear dynamics description of the extra-ocular muscles has

been proposed. This model has been extended in (Polpitiya & Ghosh, 2002; Polpitiya & Ghosh, 2003), including also a description of the soft pulleys as elastic suspensions (springs). However, this model requires that the elastic suspensions perform particular movements in order to ensure that Listing's Law is fulfilled. The model proposed in (Cannata et al., 2006; Cannata & Maggiali, 2006), and described in this section, is slightly simpler than the previous ones. In fact, it does not include the dynamics of extra-ocular muscles, since it can be shown that it has no role in implementing Listing's Law, and models soft pulleys as fixed pointwise pulleys. As it will be shown in the following, the proposed model, for its simplicity, can also be used as a guideline for the design of humanoid tendon driven robot eyes.

4.1 Geometric Model of the Eye

The eye-ball is assumed to be modeled as a homogeneous sphere of radius R, having 3 rotational degrees of freedom about its center. Extra-ocular muscles are modeled as non-elastic thin wires (Koene & Erkelens, 2004), connected to pulling force generators (Polpitiya & Ghosh, 2002). Starting from the insertion points placed on the eye-ball, the extra-ocular muscles are routed through head fixed pointwise pulleys, emulating the soft-pulley tissue. The pointwise pulleys are located on the rear of the eye-ball, and it will be shown that appropriate placement of the pointwise pulleys and of the insertion points has a fundamental role to implement the Listing's Law on a purely mechanical basis.

Let O be the center of the eye-ball, then the position of the pointwise pulleys can be described by vectors $\boldsymbol{p}_i$, while, at the primary position insertion points can be described by vectors $\boldsymbol{c}_i$, obviously assuming that $|\boldsymbol{c}_i| = R$. When the eye is rotated about a generic axis $\boldsymbol{v}$ by an angle θ, the position of the insertion points can be expressed as:

$$\boldsymbol{r}_i = R(\boldsymbol{v}, \theta)\, \boldsymbol{c}_i \quad \forall i = 1\ldots4 \tag{1}$$

where $R(\boldsymbol{v}, \theta)$ is the rotation operator from the eye to the head coordinate systems.

Each extra-ocular muscle is assumed to follow the shortest path from each insertion point to the corresponding pulley, (Demer et al., 1995); then, the path of the each extra-ocular muscle, for any eye orientation, belongs to the plane defined by vectors $\boldsymbol{r}_i$ and $\boldsymbol{p}_i$. Therefore, the torque applied to the eye by the pulling action $\tau_i \geq 0$, of each extra-ocular muscle, can be expressed by the following formula:

$$\boldsymbol{m}_i = \tau_i \frac{\boldsymbol{r}_i \times \boldsymbol{p}_i}{|\boldsymbol{r}_i \times \boldsymbol{p}_i|} \quad \forall i = 1\ldots4 \tag{2}$$

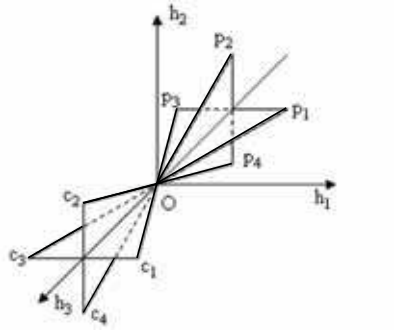

Fig. 4. The relative position of pulleys and insertion points when the eye is in the *primary position*.

From expression (2), it is clear that $|p_i|$ does not affect the direction or the magnitude of m_i so we can assume in the following that $|p_i| = |c_i|$. Instead, the orientation of the vectors p_i, called *principal directions*, are extremely important. In fact, it is assumed that p_i and c_i are symmetric with respect to the plane $\mathcal{L}$; this condition implies:

$$(v \cdot c_i) = (v \cdot p_i) \quad \forall i = 1\ldots4, \forall v \in \mathcal{L} \tag{3}$$

Finally, it is assumed that insertion points are symmetric with respect to the fixation axis:

$$(h_3 \cdot c_i) = (h_3 \cdot c_j) \quad \forall i, j = 1\ldots4 \tag{4}$$

and

$$(c_3 - c_1) \cdot (c_4 - c_2) = 0 \quad \forall i, j = 1\ldots4 \tag{5}$$

4.2 Properties of the Eye Model

In this section we review the most relevant properties of the proposed model. First, it is possible to show that, for any eye orientation compatible with Listing's Law, all the torques m_i produced by the four rectii extra-ocular muscles belong to a common plane passing through the finite rotation axis $v \in \mathcal{L}$, see (Cannata et al., 2006) for proof.

Theorem 1: Let $v \in \mathcal{L}$ be the finite rotation axis for a generic eye orientation, then there exists a plane $\mathcal{M}$, passing through v such that:

$$m_i \in \mathcal{M} \quad \forall i = 1\ldots4$$

A second important result is that, at any Listing compatible eye's orientation, the relative positions of the insertion points and pointwise pulleys form a set of parallel vectors, as stated by the following theorem, see (Cannata et al., 2006) for proof.

Theorem 2: Let $v \in \mathcal{L}$ be the finite rotation axis for a generic eye orientation, then:

$$(r_i - p_i) \times (r_j - p_j) = 0 \quad \forall i, j = 1\ldots4$$

Finally, it is possible to show that planes $\mathcal{M}$ and $\mathcal{P}_\omega$ are coincident, see (Cannata et al., 2006) for proof.

Theorem 3: Let $\mathbf{v} \in \mathcal{L}$ be the finite rotation axis for a generic eye orientation, then:

$$\mathbf{m}_i \in \mathcal{P}_\omega \quad \forall i = 1...4$$

Remark 1: Theorem (3) has in practice the following significant interpretation. For any Listing compatible eye orientation any possible torque applied to the eye, and generated using only the four *rectii* extra-ocular muscles, must lay on plane $\mathcal{P}_\omega$.

The problem now is to show, according to formula (2), when arbitrary torques $m_i \in \mathcal{P}_\omega$ can be generated using only pulling forces. Theorem 2 and theorem 3 imply that m_i are all orthogonal to the vector n_ω, normal to plane $\mathcal{P}_\omega$. Therefore, formula (2) can be rewritten as:

$$\boldsymbol{\tau} = -n_\omega \times \left(\sum_{i=1}^{4} \gamma_i \, r_i\right) \tag{6}$$

where:

$$\gamma_i = \frac{\tau_i}{|n_\omega \times r_i|} \geq 0 \quad \forall i = 1\ldots4 \tag{7}$$

take into account the actual pulling forces generated by the extra-ocular muscles. From formula (6), it is clear that $\boldsymbol{\tau}$ is orthogonal to a *convex* linear combination of vectors r_i. Then,

it is possible to generate any torque vector laying on plane $\mathscr{P}_\omega$, as long as $\boldsymbol{n}_\omega$ belongs to the convex hull of vectors $\boldsymbol{r}_i$ as shown in Fig. 5.

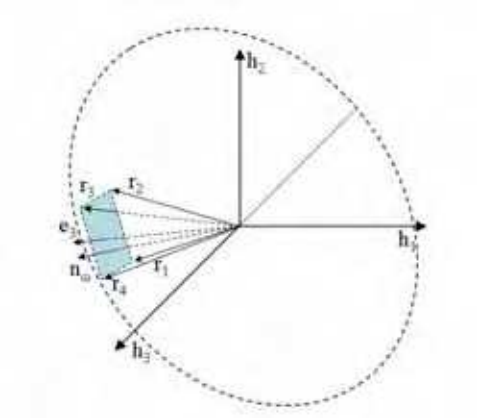

Fig. 5. When vector $\boldsymbol{n}_\omega$ belongs to the convex hull of vectors $\boldsymbol{r}_i$ then rectii extra-ocular muscles can generate any admissible torque on P_ω.

Remark 2: The discussion above shows that the placement of the insertion points affects the range of admissible motions. According to the previous discussion when the eye is in its primary position any torque belonging to plane $\mathscr{L}$ can be assigned. The angle β formed by the insertion points with the optical axis determines the actual eye workspace. For an angle $\beta = 55\ deg$ the eye can rotate of about $45\ deg$ in all directions with respect to the direction of fixation at the primary position.

Assume now that, under the assumptions made in section 3, a simplified dynamic model of the eye could be expressed as:

$$I\dot{\omega} = \boldsymbol{\tau} \tag{8}$$

where I is a scalar describing the momentum of inertia of the eye-ball, while $\dot{\omega}$ is its angular acceleration of the eye. Let us assume at time 0 the eye to be in the primary position, with zero angular velocity (zero state). Then, the extra-ocular muscles can generate a resulting torque of the form:

$$\boldsymbol{\tau} = \boldsymbol{v}\,\theta(t) \tag{9}$$

where $\boldsymbol{v} \in \mathscr{L}$ is a constant vector and $\theta(t)$ a scalar control signal. Therefore, ω and $\dot{\omega}$ are parallel to $\boldsymbol{v}$; then, it is possible to reach any Listing compatible orientation, and also, during the rotation, the Half Angle Rule is satisfied. Similar reasoning can be applied to control the eye orientation to the primary position starting from any Listing compatible orientation and zero angular velocity.

The above analysis proves that saccadic motions from the primary position to arbitrary secondary positions can be implemented on a mechanical basis. However, simulative examples, discussed in (Cannata & Maggiali, 2006), show that also generic saccadic motions can be implemented adopting the proposed model. Theoretical investigations on the model properties are currently ongoing to obtain a formal proof of the evidence provided by the simulative tests.

5. Robot Eye Design

In this section we will give a short overview of a prototype of humanoid robot eye designed following the guidelines provided by the model discussed in the previous section, while in the next sections we will discuss the most relevant design details related to the various modules or subsystems.

5.1 Characteristics of the Robot

Our goal has been the design of a prototype of a robot eye emulating the mechanical structure of the human eye and with a comparable working range. Therefore, the first and major requirement has been that of designing a spherical shape structure for the eye-ball and to adopt a tendon based actuation mechanism to drive the ocular motions. The model discussed in the previous sections allowed to establish the appropriate quantitative specifications for the detailed mechanical design of the system.
At system level we tried to develop a fairly integrated device, keeping also into account the possible miniaturization of the prototype to human scale. The current robot eye prototype has a cylindrical shape with a diameter of about *50 mm* and an overall length of about *100 mm*, Fig. 6*;* the actual eye-ball has a diameter of *38.1 mm* (i.e. about 50% more than the human eye). These dimensions have been due to various trade-offs during the selection of the components available off-the-shelf (e.g. the eye-ball, motors, on board camera etc.), and budget constraints.

5.2 Components and Subsystems.

The eye robot prototype consists of various components and subsystems. The most relevant, discussed in detail in the next sections, are: the eye-ball, the eye-ball support, the pointwise pulleys implementation, the actuation and sensing system, and the control system architecture.

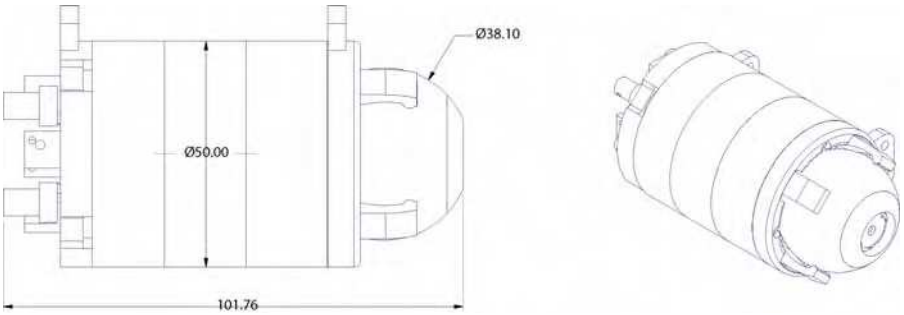

Fig. 6. Outline of the robot eye.

The design of the eye-ball and its support structure, has been inspired by existing ball transfer units. To support the eye-ball it has been considered the possibility of using thrust-bearings, however, this solution has been dropped since small and light components for a miniature implementation (human sized eye), were not available. The final design has been based on the implementation of a low friction (PTFE) slide bearing, which could be easily scaled to smaller size.
The actuation is performed by tendons, i.e. thin stiff wires, pulled by *force generators*. The actuators must provide a linear motion of the tendons with a fairly small stroke (about *30*

mm, in the current implementation, and less than *20 mm* for an eye of human size), and limited pulling force. In fact, a pulling force of *2.5 N* would generate a nominal angular acceleration of about *6250 rad sec*$^{-2}$, for an eye-ball with a mass *50 g* and radius of *20 mm*, and about *58000 rad sec*$^{-2}$ in the case of an eye of human size with a mass of *9 g* and radius of *12 mm*. The actuators used in the current design are standard miniature DC servo motors, with integrated optical encoder, however, various alternative candidate solutions have been taken into account including: shape memory alloys and artificial muscles. According to recent advances, (Carpi et al., 2005; Cho & Asada, 2005), these technologies seem very promising as alternative solutions to DC motors mostly in terms of size and mass (currently the mass of the motors is about *160 g*, *i.e.* over *50%* of the total mass of the system, without including electronics). However, presently both shape memory alloys and artificial muscles require significant engineering to achieve operational devices, and therefore have not be adopted for the first prototype implementation.
In the following the major components and subsystems developed are reviewed.

6. The Eye-Ball

The eye ball is a precision PTFE sphere having a diameter of 38.1 *mm* (1.5*in*). The sphere has been CNC machined to host a commercial CMOS camera, a suspension spring, and to route the power supply and video signal cables to the external electronics. A frontal flange is used to allow the connection of the tendons at the specified insertion points, and to support miniature screws required to calibrate the position of the camera within the eye ball. On the flange it is eventually placed a spherical cover purely for aesthetical reasons. Fig. 7 and Fig. 8 show the exploded view and the actual eye-ball.

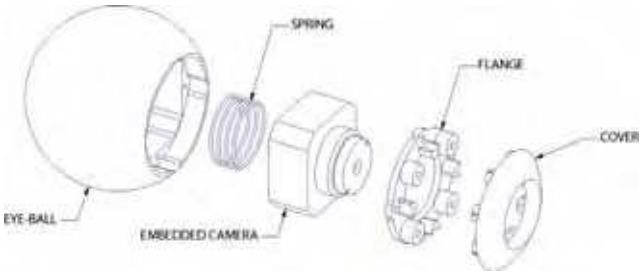

Fig. 7. Exploded view of the eye-ball.

Fig. 8. The machined eye-ball (left), and the assembled eye-ball (camera cables shown in background).

The insertion points form an angle of *55 deg*, with respect to the (geometric) optical axis of the eye, therefore the eye-ball can rotate of about *45 deg* in all directions. The tendons used are monofiber nylon coated wires having a nominal diameter of *0.25 mm*, well approximating the geometric model proposed for the extra-ocular muscles.

7. Supporting Structure

The structure designed to support the eye ball is formed by two distinct parts: a low friction support, designed to hold the eye ball, Fig. 9, and a rigid flange used to implement the pointwise pulleys, and providing appropriate routing of the actuation tendons) required to ensure the correct mechanical implementation of Listing's Law, Fig. 13.

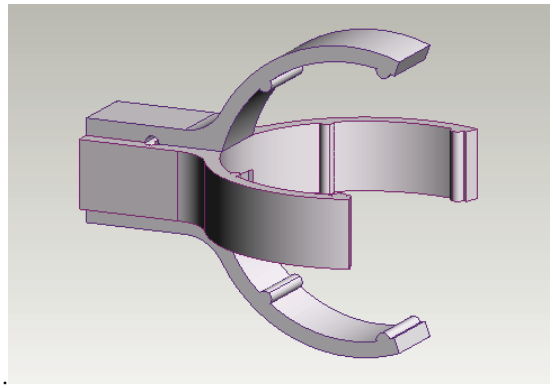

Fig. 9. CAD model of the eye-ball support (first concept).

7.1 The Eye-Ball Support

The eye-ball support is made of two C-shaped PTFE parts mated together, Fig. 10**.** The rear part of the support is drilled to allow the routing of the power supply and video signal cables to and from the on board camera.

The eight *bumps* on the C-shaped parts are the actual points of contact with the eye-ball. The placement of the contact points has been analysed by simulation in order to avoid interference with the tendons. Fig. 11 shows the path of one insertion point when the eye is rotated along the boundary of its workspace (i.e. the fixation axis is rotated to form a cone with amplitude of *45 deg*). The red marker is the position of the insertion point at the primary position while the green markers represent the position of two frontal contact points. The *north pole* in the figure represents the direction of axis $\boldsymbol{h}_3$. The frontal bumps form an angle of *15 deg* with respect to the *equatorial* plane. The position of the rear bumps is constrained by the motion of the camera cables coming out from the eye-ball. To avoid interferences the rear bumps form an angle of *35 deg* with respect to *equatorial* plane of the eye.

7.2 The Pointwise Pulleys

The rigid flange, holding the eye-ball support, has the major function of implementing the pointwise pulleys. The pulleys have the role of constraining the path of the tendons so that, at every eye orientation, each tendon passes through a given head fixed point belonging to the principal direction associated with the corresponding pointwise pulley.

Let us assume the eye in a Listing compatible position A, then we may assume that a generic tendon is routed as sketched in Fig. 12. The pulley shown in the figure is tangent to the principal direction at point $\boldsymbol{p}_i$, and it allows the tendon to pass through $\boldsymbol{p}_i$. Assume now to rotate the eye to another Listing compatible position B; if the pulley could tilt about the principal axis, during the eye rotation, the tangential point $\boldsymbol{p}_i$ would remain the same so that the tendon is still routed through point $\boldsymbol{p}_i$. Therefore, the idea of the pulley tilting (about the principal axis) and possibly rotating (about its center), fully meets the specifications of the pointwise pulleys as defined for the eye model.

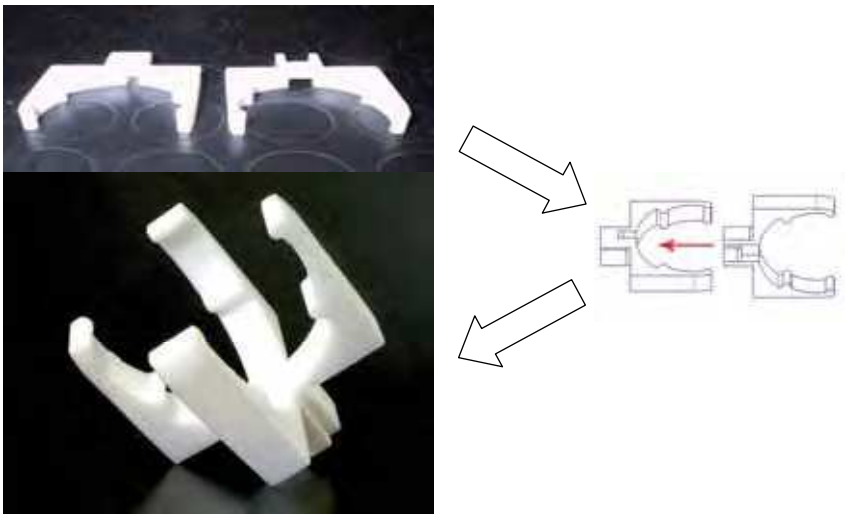

Fig. 10. The eye-ball support is formed by two PTFE parts mated together (final design).

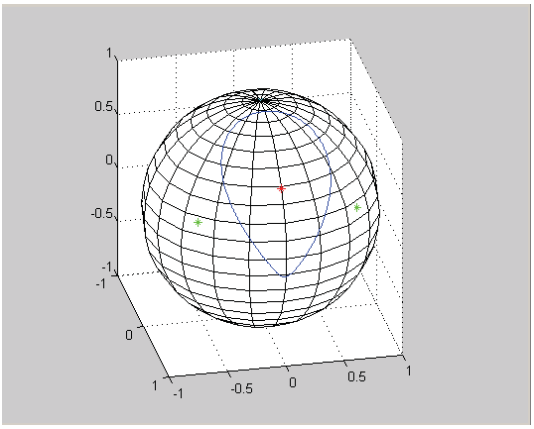

Fig. 11. During Listing compatible eye motions, the insertion points move within the region internal to the blue curve. The red marker represents the position of the insertion point at the primary position, while the green markers are the positions of (two of) the frontal contact points on the eye-ball support. The fixation axis at the primary position, $\boldsymbol{h}_3$, points upward.

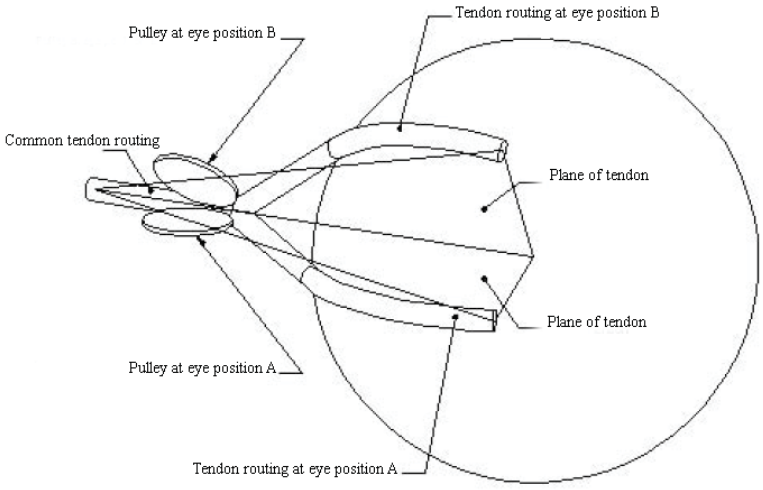

Fig. 12. Sketch of the tendon's paths, showing the tilting of the routing pulley when the eye is rotated from position *A* to position *B* (tendons and pulleys diameters not to scale).

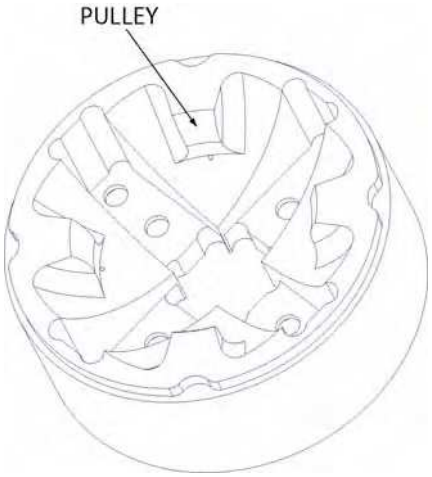

Fig. 13. Detail of the flange implementing the pointwise pulleys. The tendon slides along a section of a toroidal surface.

A component featuring these characteristics could be implemented, but its miniaturization and integration has been considered too complex, so we decided to implement a *virtual pulley*, to be intended as the surface formed by the envelope of all the tilting pulleys for all the admissible eye orientations. Since the pulley tilts about the principal axis at point $\boldsymbol{p}_i$, then the envelope is a section of a torus with inner diameter equal to the radius of the tendon, and external radius equal to the radius selected for the pulley. Then, the implementation of the virtual pulley has been obtained by machining a section of a torus on the supporting flange as shown in Fig. 13.
The assembly of the eye-ball and its supporting structure is shown in Fig. 14.

8. Sensing and Actuation

The robot-eye is actuated by four DC servo-motors, producing a maximum output torque of *12 mNm,* and pulling four independent tendons routed to the eye as discussed in the previous section. The actuators are integrated within the structure supporting the eye, as shown in Fig. 15 and Fig. 16.

Fig. 14. The eye-ball and its supporting parts.

Fig. 15. Four DC motor actuate the tendons; pulleys route the tendons towards the eye-ball

The servo-motors are equipped with optical encoders providing the main feedback for the control of the ocular movements. A second set of sensors for measuring the mechanical tension of the tendons is integrated in the robot. In fact, as the tendons can only apply pulling forces, control of the ocular movements can be properly obtained only if slackness of the tendons or their excessive loading is avoided. The tension sensors are custom made and integrated within the supporting structure of the eye, Fig. 17.
Each sensor is formed by an infrared led/photodiode couple separated by a mobile *shutter*, preloaded with a phosphore-bronze spring. As shown in Fig. 18, the tension of the tendon counter-balances the pre-load force thus varying the amount of IR radiation received. The sensor output is the current generated by the photodiode according to the following equation:

$$I_p = k_p \gamma(f) E0 \tag{10}$$

where I_p is the current generated by the photodiode, k_p is the characteristic parameter of the photodiode, $E0$ is the IR radiation emitted by the led, and $\gamma(f)$ is a monotonic non-linear function of the tendon's tension depending on the system geometry. Each sensor is calibrated and a look-up table is used to map its current to tension characteristic.

Fig. 16. The body of the MAC-EYE robot. All the motors are integrated within the body; furthermore, all the cables from and to the eye-ball and the embedded optical tension sensors are routed inside of the structure.

Fig. 17. Implementation of the embedded sensors for measuring the mechanical tension of the tendons. The picture shows the *shutter* and its preloading spring, cables and tendons.

9. Robot Control System

9.1 The control architecture

The control architecture is implemented as a two level hierarchical system. At low level are implemented two control loops for each actuator. In the first loop a P-type control action regulates the tension of the *i-th* tendon at some constant reference value f_i^*, while in the second loop a PI-type action controls the motor velocity as specified by signal $\dot{\bar{q}}_i^*$, see Fig. 19. The tension feedback control loop makes the eye-ball backdrivable, so the eye can be positioned *by hand*. Both the reference signals $\dot{\bar{q}}_i^*$ and f_i^* are generated by the higher level control modules which implement a position based PI-type controller.

Currently, the major task implemented is that of controlling the eye position during emulated saccadic movements. Therefore, coordinated signals q_i^* and $\dot{q}_i^*$ must be generated for all the actuators. In order to compute the appropriate motor commands a geometric and a kinematic eye model are implemented as described below.

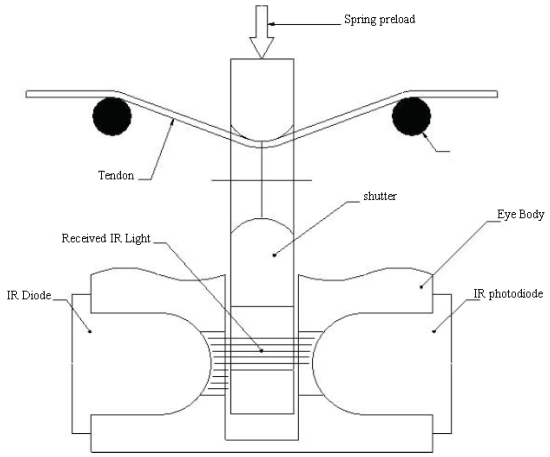

Fig. 18. Sketch of the tension sensor (not to scale).

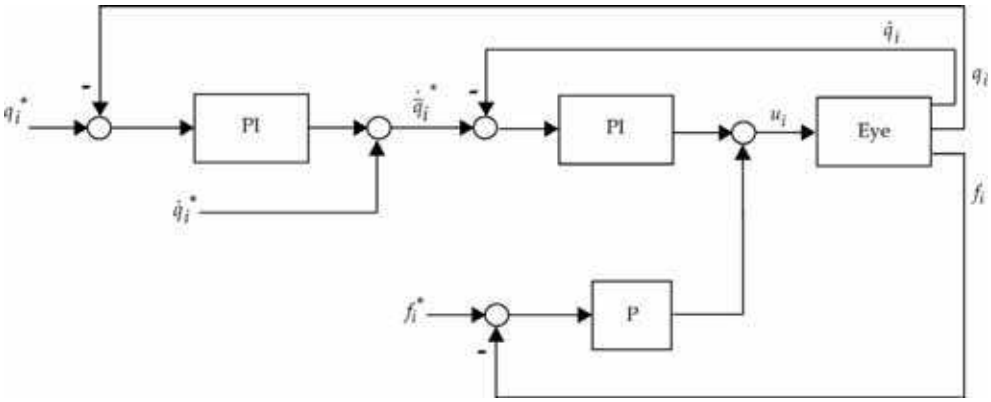

Fig. 19. Robot eye control scheme. The picture shows the control loops related to a single actuator.

Assume that a given reference trajectory for the eye is given and expressed by a rotation matrix $R^*(t)$, and an angular velocity $\omega^*(t)$. Then, an algebraic and a differential mapping, relating the eye orientation to the displacement of the tendons, can be easily computed. In fact, as shown in Fig. 20, for a given eye orientation the tendon starting from the insertion point $\boldsymbol{r}_i$ remains in contact with the eye-ball up to a point $\boldsymbol{t}_i$ (point of tangency). From $\boldsymbol{t}_i$ the tendon reaches the pointwise pulley and then moves towards the motor which provides the actuation force. For a given position of the eye there exists a set of displacements of the *free end* of the tendons corresponding to the amount of rotation to be commanded to the motors. According to Fig. 20, for each tendon this amount can be computed (with respect to a reference eye position, e.g. the primary position), using the formula:

$$x_i = R(\phi_i - \phi_{0i}) \tag{11}$$

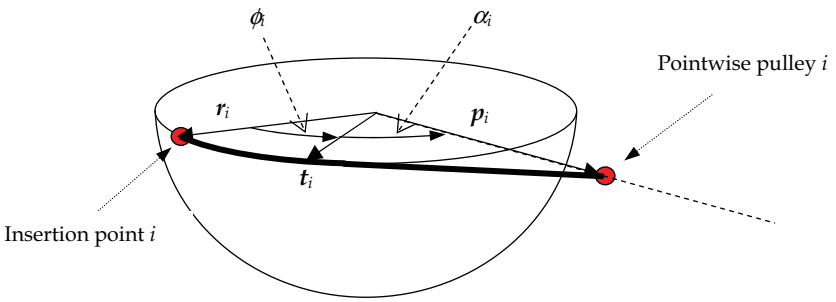

Fig. 20. The plane of tendon i for a generic eye orientation. Angle α_i is constant for any eye orientation.

where x_i is the amount of displacement of the *free end* of the tendon, while ϕ_i and ϕ_{0i} are the angles (with positive sign), formed by vectors $\boldsymbol{r}_i$ and $\boldsymbol{t}_i$ at a generic eye orientation, and at the primary position, respectively. Signs are chosen so that if $x_i < 0$ then the corresponding tendon must be pulled in order to orient the eye as specified by matrix $R^*(t)$. In order to compute x_i the angle ϕ_i can be determined, as follows. According to Fig. 20, the angle α_i must be constant for any eye orientation and can be expressed as:

$$\alpha_i = \cos^{-1}\left(\frac{R}{d_i}\right) \tag{12}$$

If the eye orientation is known with respect to frame <*h*>, then $\boldsymbol{r}_i$ is known, hence:

$$Rd_i \cos(\alpha_i + \phi_i) = \boldsymbol{r}_i \cdot \boldsymbol{p}_i \tag{13}$$

and finally, from equations (12) and (13), we obtain:

$$\phi_i = \cos^{-1}\left(\frac{\boldsymbol{r}_i \cdot \boldsymbol{p}_i}{Rd_i}\right) - \cos^{-1}\left(\frac{R}{d_i}\right) \tag{14}$$

The time derivative of ϕ_i can be computed by observing that $\dot{\boldsymbol{r}}_i = \omega \times \boldsymbol{r}_i$, where ω is the angular velocity of the eye, then, the time derivative of equations (13) can be written as:

$$\frac{d}{dt}(\boldsymbol{r}_i \cdot \boldsymbol{p}_i) = -Rd_i \sin(\alpha_i + \phi_i)\dot{\phi}_i \tag{15}$$

Therefore, we obtain the following equality:

$$(\omega \times \boldsymbol{r}_i) \cdot p_i = -Rd_i \sin(\alpha_i + \phi_i)\dot{\phi}_i \tag{16}$$

Then, by observing that $(\omega \times \boldsymbol{r}_i) \cdot p_i = (\boldsymbol{r}_i \times p_i) \cdot \omega$, we have:

$$\dot{\phi}_i = -\frac{1}{|\boldsymbol{r}_i \times p_i|}(\boldsymbol{r}_i \times p_i) \cdot \omega \tag{17}$$

Then, if $R^*(t)$ and $\omega^*(t)$ are the desired trajectory and angular velocity of the eye, the reference motor angles and velocities can be computed using formulas (11), (14) and (17) as:

$$
\begin{aligned}
q_i^*(t) &= \frac{R}{R_m}\left[\cos^{-1}\left(\frac{\boldsymbol{r}_i^* \cdot \boldsymbol{p}_i}{R d_i}\right) - \cos^{-1}\left(\frac{R}{d_i}\right) - \phi_{i0}\right] \\
\dot{q}_i^*(t) &= -\frac{R}{R_m}\frac{1}{\left|\boldsymbol{r}_i^* \times p_i\right|}\left(\boldsymbol{r}_i^* \times p_i\right)\cdot \omega^*
\end{aligned}
\tag{18}
$$

where R_m is the radius of the motor pulley.

9.2 The control architecture

The computer architecture of the robot eye is sketched in Fig. 23. A PC based host computer implements the high level position based control loop and the motor planning algorithm (18). Currently the high level control loop runs at a rate of *125 Hz*.

The low level control algorithms are implemented on a multi-controller custom board, Fig. 21, featuring four slave micro-controllers (one for each motor), operating in parallel and coordinated by a master one managing the communications through CAN bus with higher level control modules or other sensing modules (e.g. artificial vestibular system). The master and slave microcontrollers communicates using a multiplexed high speed (*10 Mbits*) serial link and operate at a rate of 1.25*KHz*.

Fig. 21. The prototype custom embedded real-time controller. The board has dimensions of 69 × 85mm^2.

Fig. 22. Complete stereoscopic robot system

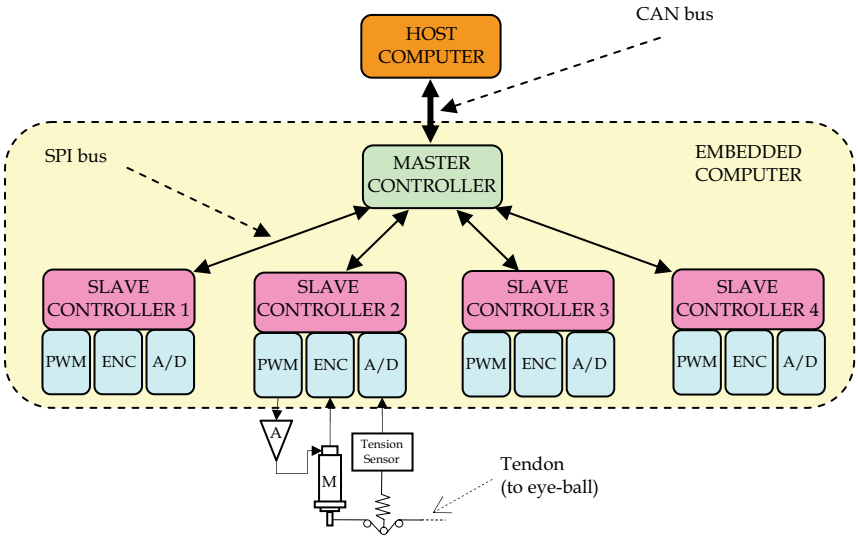

Fig. 23. Sketch of the computer control architecture.

10. Conclusions

This chapter has shown the feasibility of a tendon driven robot eye featuring the implementation of Listing's Law on a mechanical basis. The design of the robot is based on a model which is strongly inspired on assumptions derived from physiological evidence.
The achievements discussed in this chapter represent the starting point for the development of a more complex humanoid robot eye. From the mechanical point of view the most important advancement is represented by the possibility of extending the actuation to six tendons in order to enable the implementation of more complex ocular motions as the *vestibulo-ocular reflex*. From a theoretical point of view a more complete analysis of the properties of the proposed eye model could provide further understanding of the dynamics of saccadic motions. Furthermore, other issues such as eye miniaturization and embedding of image processing algorithms modules for direct visual feedback represent important challenges for the development of fully operational devices.

11. References

Albers, A. ; Brudniok, S. & Burger, W. (2003). The Mechanics of a Humanoid, *Proceedings of Humanoids 2003*, ISBN 3-00-012047-5; Karlsruhe, September 2003, IEEE, Germany.

Angelaki, D. E. & Hess, B. J. M., (2004). Control of eye orientation: where does the brain's role ends and the muscles begins, *European Journal of Neurosciences*, vol. 19, pp. 1-10, 2004, ISSN 0270-6474.

Becker, W. (1991). Eye Movements, *Carpenter, R.H.S. ed., Macmillan*, pp. 95-137,1991, ISSN 0301-4738.

Biamino, D. & Piazza, A. (2005). Studio Progetto e Realizzazione di una Coppia di Occhi Robotici con Sistema di Controllo Embedded, *Master Degree Thesis*, Faculty of Engineering, University of Genova, 2005, no ISBN or ISSN.

Cannata, G. ; D'Andrea, M.; Monti, F. & Maggiali, M. (2006). Implementation of Listing's Law for a Robot Eye, *Proceedings of Sy.Ro.Co 2006*, Bologna (Italy), Sept. 6-8, no ISBN or ISSN, 2006.

Cannata, G. & Maggiali, M. (2006). Implementation of Listing's Law for a Tendon Driven Robot Eye, *Proceedings of. IEEE Conf. on Intelligent Robots and Systems, IROS 2006*, pp. 3940-3945, ISBN 1-4244-0259-X, Beijing, Oct. 9-15, 2006, IEEE, China.

Clark, R. A.; Miller, J.M. & Demer, J. L. (2000). Three-dimensional Location of Human Rectus Pulleys by Path Inflection in Secondary Gaze Positions, *Investigative Ophthalmology and Visual Science*, vol. 41, pp. 3787-3797, 2000, ISSN 0146-0404.

Carpi F.; Migliore A.; Serra G. & De Rossi, D. (2005). Elical Dielectric Elastomer Actuators, *Smart Material and Structures*, vol. 14, pp. 1210-1216, 2005, ISSN 0964-1726.

Cho, K. & Asada, H. H. (2005). Segmentation theory for design of a multi-axis actuator array using segmented binary control. *Proceedings of the American Control Conference*, vol. 3, pp. 1969-1974, ISBN 0-7803-649*, ACC*, 2005.

Demer, J. L.; Miller J. M.; Poukens V.; Vinters, H. V. & Glasgow B.J. (1995). Evidence for fibromuscular pulleys of the recti extraocular muscles, *Investigative Ophthalmology and Visual Science*, vol. 36, pp. 1125-1136, 1995, ISSN 0030-3747.

Demer, J. L.; Ho, S. Y. & Pokens, V. (2000). Evidence for Active Control of Rectus Extraocular Muscle Pulleys, *Invest. Ophtalmol. Visual Sci.*, vol. 41, pp. 1280-1290, 2000, ISSN 0042-6989.

Furman, J. M. & Schor, R. (2003). Orientation of Listing's plane during static tilt in young and older human subjects, *Vision Res.*, vol. 43, pp. 67-76, 2003, ISSN 0042-6989.

Gu, J.; Meng, M., Cook, A. & Faulkner, M. G. (2000). A study of natural movement of artificial eye plant. *Robotics and Autonomous System*, vol. 32, pp. 153-161 , 2000, ISSN 0921-8890.

Haslwanter, T. (1995). Mathematics of Three-dimensional Eye Rotations, *Vision Res.*, vol. 35, pp. 1727-1739, 1995, ISSN 0042-6989.

Haslwanter, T. (2002). Mechanics of Eye Movements Implications of the Orbital Revolution, *Ann. N. Y. Acad. Sci.*, vol. 956, pp. 33-41, ,2002, ISSN 0077-8923.

Hepp, K. (1994). Oculomotor control: Listing's law and all that, *Current Opinion in Neurobiology*, vol. 4, pp. 862-868, 1994 ISSN 0959-4388.

Koene, A. R. & Erkelens, C.J. (2004). Properties of 3D rotations and their relation to eye movement control, *Biol. Cybern.*, vol. 90, pp. 410-417, Jul. 2004, ISSN 0340-1200.

Koornneef, L. (1974). The first results of a new anatomical method of approach to the human orbit following a clinical enquiry, *Acta Morphol Neerl Scand*, vol. 12, n. 4, pp. 259-282, 1974, ISSN 0001-6225.

Lockwood-Cooke, P.; Martin, C. F. & Schovanec L. (1999). A Dynamic 3-d Model of Ocular Motion, *Proceedings of 38th Conference of Decision and Control*, ISBN 0-7803-5253-X, Phoenix, December,1999.

Miller, J. M. & Robinson, David A. (1984). A Model of the Mechanics of Binocular Alignment. *Computer and Biomedical Research,* vol.17, pp. 436-470, 1984, ISSN 0010-4809.

Miller, J. M. (1989). Functional anatomy of normal human rectus muscles, *Vision Res.*, pp. 223-240, vol. 29, 1989, ISSN 0042-6989.

Polpitiya, A. D. & Ghosh, B. K. (2002). Modelling and Control of Eye-Movements with Muscolotendon Dynamics, *Proceedings of American Control Conference*, pp. 2313-2318, ISBN 1902815513, Anchorage, May 2002.

Polpitiya, A. D. & Ghosh, B. K. (2003). Modeling the Dynamics of Oculomotor System in Three Dimensions, *Proceedings of Conference on Decision and Control*, pp. 6418-6422, ISBN 0-7803-7925-X, Maui, Dec. 2003.

Polpitiya, A. D.; Ghosh, B. K., Martin, C. F. & Dayawansa, W. P. (2004). Mechanics of the Eye Movement Geometry of the Listing Space, *Proceedings of American Control Conference*, ISBN 0-444-81933-9, 2004.

Pongas, D., Guenter, F., Guignard, A. & Billard, A. (2004). Development of a Miniature Pair of Eyes With Camera for the Humanoid Robot Robota, *Proceedings of IEEE-RAS/RSJ International Conference on Humanoid Robots – Humanoids 2004*, vol. 2, pp. 899- 911, ISBN 0-7803-8863-1,Santa Monica, Los Angeles, 2004.

Porrill, J.; Warren, P. A. & Dean, P., (2000). A simple control law generates Listing's positions in a detailed model of the extraocular muscle system, *Vision Res.*, vol. 40, pp. 3743-3758, 2000, ISSN 0042-6989.

Quaia, C. & Optican, L. M. (1998). Commutative Saccadic Generator Is Sufficient to Control a 3D Ocular Plant With Pulleys, *The Journal of Neurophysiology*, pp. 3197-3215, vol. 79, 1998, ISSN 0022-3077.

Raphan, T. (1998). Modeling Control of Eye Orientation in Three Dimensions. I. Role of Muscle Pulleys in Determining Saccadic Trajectory, *The Journal of Neurophysiology*, vol. 79, pp. 2653-2667, 1998, ISSN 0022-3077.

Robinson, D. A., (1991). Overview, In: *Carpenter, R.H.S. ed., Macmillan* ,pp. 320-332,1991, ISSN 0301-4738.

Straumann D.; Zee. D. S.; Solomon D. & Kramer P. D., (1996). Validity of Listing's law during fixations, saccades, smooth pursuit eye movements, and blinks, *Exp. Brain Res.*, vol. 112, pp. 135-146, 1996, ISSN 0014-4819.

Sparks D. L. (2002). The brainstem control of saccadic eye movements. *Nature Rev.*, vol. 3, pp. 952-964, December, 2002, ISSN 1471-003X.

Tweed, D. & Vilis, T. (1987). Implications of Rotational Kinematics for the Oculomotor System in Three dimensions, *The Journal of Neurophysiology,* vol. 58, no.4, pp. 832-849, Oct. 1987, ISSN 0022-3077.

Tweed D. & Vilis T., (1988). Rotation Axes of Saccades, *Ann. N. Y. Acad. Sci.*, vol. 545, pp. 128-139, 1988, ISSN 0077-8923.

Tweed D. & Vilis T., (1990). Geometric relations of eye position and velocity vectors during saccades, *Vision. Res.*, vol. 30, n. 1, pp. 111-127, 1990, ISSN: 0042-6989.

Wong, A. M. F.; Tweed D. & Sharpe, J. A., (2002). Adaptive Neural Mechanism for Listing's Law Revealed in Patients with Sixth Nerve Palsy, *Investigative Ophtalmology and Visual Science*, vol. 43, n. 1, pp. 112-118, Jan. 2002, ISSN 0146-0404.

Humanoid Robots: New Developments

Edited by Armando Carlos de Pina Filho

ISBN 978-3-902613-00-4

Hard cover, 582 pages

Publisher I-Tech Education and Publishing

Published online 01, June, 2007

Published in print edition June, 2007

For many years, the human being has been trying, in all ways, to recreate the complex mechanisms that form the human body. Such task is extremely complicated and the results are not totally satisfactory. However, with increasing technological advances based on theoretical and experimental researches, man gets, in a way, to copy or to imitate some systems of the human body. These researches not only intended to create humanoid robots, great part of them constituting autonomous systems, but also, in some way, to offer a higher knowledge of the systems that form the human body, objectifying possible applications in the technology of rehabilitation of human beings, gathering in a whole studies related not only to Robotics, but also to Biomechanics, Biomimmetics, Cybernetics, among other areas. This book presents a series of researches inspired by this ideal, carried through by various researchers worldwide, looking for to analyze and to discuss diverse subjects related to humanoid robots. The presented contributions explore aspects about robotic hands, learning, language, vision and locomotion.

How to reference

In order to correctly reference this scholarly work, feel free to copy and paste the following:

Giorgio Cannata and Marco Maggiali (2007). Design of a Humanoid Robot Eye, Humanoid Robots: New Developments, Armando Carlos de Pina Filho (Ed.), ISBN: 978-3-902613-00-4, InTech, Available from: http://www.intechopen.com/books/humanoid_robots_new_developments/design_of_a_humanoid_robot_eye

INTECH
open science | open minds

InTech Europe
University Campus STeP Ri
Slavka Krautzeka 83/A
51000 Rijeka, Croatia
Phone: +385 (51) 770 447
Fax: +385 (51) 686 166
www.intechopen.com

InTech China
Unit 405, Office Block, Hotel Equatorial Shanghai
No.65, Yan An Road (West), Shanghai, 200040, China
中国上海市延安西路65号上海国际贵都大饭店办公楼405单元
Phone: +86-21-62489820
Fax: +86-21-62489821